Proc. of the European Safety and Reliability Conference (ESREL 2026)
Edited by José C. Matos, Paulo B. Lourenço, Michael Beer, Daniel Oliveira, Edoardo Patelli, Hélder S. Sousa, Rui A. Silva and Monica Santamaria

doi: 10.3850/ESREL2026061419_esrel26-p27692-cd

Environmental and Economic Assessment of a Reliability-Based Design Model for FRP-Confined Concrete Columns

Amirhossein Mohammadi

ISISE, Dept. of Civil Engineering, Univ. of Minho, Azurém, Guimarães, Portugal.
E-mail: Amirh.Mohammadi@civil.uminho.pt

Javad Shayanfar

ISISE, Dept. of Civil Engineering, Univ. of Minho, Azurém, Guimarães, Portugal.
E-mail: arch3d.ir@gmail.com

Joaquim António Oliveira Barros

ISISE, Dept. of Civil Engineering, Univ. of Minho, Azurém, Guimarães, Portugal.
E-mail: barros@civil.uminho.pt

The recent development of a reliability-based design (RBD) framework for fibre-reinforced polymer (FRP)-confined concrete columns has significantly advanced the safety calibration and efficiency of confinement models through probabilistic formulations of resistance factors. However, the broader implications of such reliability-informed designs on sustainability and cost-effectiveness remain largely unexplored. This study extends the RBD model proposed by Mohammadi et al. (2025) by quantifying its environmental and economic impacts in comparison with the conventional design provisions of *f*ib Bulletin 90 and ACI 440.2R. The analysis integrates life-cycle assessment (LCA) and an initial cost analysis to quantify the environmental and economic impacts. Three representative column geometries (circular, square, and rectangular) are analysed across a range of strength improvement levels (0-100%). Results indicate that the RBD-calibrated model reduces FRP material demand by up to 100% (where confinement is deemed unnecessary given that the less conservative partial factor provided by this model gives a higher unconfined design concrete strength value compared to other models) and provides consistent savings of over 40% compared to *f*ib and ACI provisions for circular sections. It also maintains material efficiency advantages for geometrically challenging rectangular sections at moderate strengthening levels, all while maintaining the target reliability index ($\beta_T = 3.8$). This translates to significant reductions in embodied carbon emissions and construction costs. The findings emphasise that incorporating reliability-based calibration into design practice not only ensures code-compliant safety margins but also contributes substantially to the environmental and economic sustainability of FRP-based strengthening systems.

Keywords: Reliability-based design, FRP-confined concrete, probabilistic modelling, life-cycle assessment, initial cost analysis, structural reliability, sustainable infrastructure.

1. Introduction

The rehabilitation and retrofitting of existing reinforced concrete (RC) infrastructure constitutes one of the most pressing challenges in modern civil engineering. Ageing structures worldwide face deterioration due to corrosion, inadequate design provisions, increased service loads, and environmental degradation [1]. Within this context, the external bonding of Fibre-Reinforced Polymer (FRP) composites has established itself as a paramount solution for structural strengthening due to its high strength-to-weight ratio, corrosion resistance, ease of application, and design flexibility.

However, the widespread adoption of FRP strengthening systems faces several challenges. Current design provisions such as *f*ib Bulletin 90 and ACI 440.2R rely on deterministic partial factors that, while providing a rational framework, may not fully capture the complex non-linear interactions between confinement stiffness, cross-sectional geometry, and material properties. These fixed partial factors often lead to conservative designs that, while ensuring safety, can result in significant material waste and associated environmental and economic burdens [1].

Recent advances in reliability-based design (RBD) frameworks offer a rational alternative. By calibrating resistance factors based on probabilistic analysis and target reliability indices, RBD approaches can optimise material usage while maintaining consistent safety levels across different design scenarios [1]. However, the sustainability implications of such optimisation remain largely unexplored.

This study addresses this gap by conducting a comprehensive environmental and economic assessment of the RBD model developed by Mohammadi et al. (2025). Specifically, we:

- Compare the material demands of the RBD model against *f*ib Bulletin 90 and ACI 440.2R for three representative column geometries
- Quantify the environmental impact through life-cycle assessment (LCA) focusing on Global Warming Potential (GWP)
- Evaluate economic performance through initial cost analysis of capital and installation expenditures
- Demonstrate the sustainability benefits of reliability-informed design optimization

2. Background

2.1. *Mechanics of FRP Confinement*

The fundamental mechanism of FRP-confined concrete relies on passive lateral restraint. Under axial compression, the concrete core dilates due to Poisson's effect, activating tensile hoop stresses in the FRP jacket. This lateral confinement pressure suppresses microcracking and enhances both strength and ductility.

The confining pressure (f_l) can be generalised for any section geometry using the concept of equivalent diameter (D^*):

$$f_\mathrm{l} = \frac{2E_\mathrm{f}\varepsilon_\mathrm{fe}t_\mathrm{f}}{D^*} \tag{1}$$

where E_f is the elastic modulus of FRP, ε_fe is the effective confinement strain, t_f is the effective FRP thickness ($n^k \cdot t_\mathrm{ply}$) where k in *f*ib Bulletin 90 and the RBD model is equal to 0.85 if $n_\mathrm{f} \geq 4$ and 1 otherwise, and D^* is the equivalent diameter of the section. For circular columns, D^* is equal to the diameter D, while for non-circular sections, it is defined according to the specific design code formulation.

There is a distinction between circular and non-circular sections. In non-circular sections, arching action concentrates effective confinement at rounded corners, leaving mid-height sections of flat sides largely unconfined. Accordingly, This geometric inefficiency is quantified through shape effectiveness factors that depend on the corner radius ratio ($2r_\mathrm{c}/b$) and aspect ratio (h/b).

2.2. *Design Code Provisions*

2.2.1. *fib Bulletin 90*

The *f*ib Bulletin 90 approach [2] incorporates partial factors and detailed geometric considerations:

$$f_\mathrm{ccd} = f_\mathrm{cd} + 3.3 \cdot \left(\frac{b}{h}\right)^2 \cdot \alpha_\mathrm{f} \cdot f_\mathrm{l} \tag{2}$$

$$D^* = \frac{2bh}{b+h} \quad \text{(for rectangular sections)} \tag{3}$$

α_f accounts for section shape, wrapping continuity and fibre orientation effects and equals to:

$$\alpha_\mathrm{f} = \alpha_\mathrm{n} \cdot \alpha_\mathrm{s} \cdot \alpha_\mathrm{a} \tag{4}$$

where,

$$\alpha_\mathrm{n} = 1 - \frac{(b-2r_\mathrm{c})^2 + (h-2r_\mathrm{c})^2}{3A_\mathrm{g}} \tag{5}$$

$$A_\mathrm{g} = \begin{cases} \pi\frac{D^2}{4} & \text{Circular} \\ bh & \text{Rectangular} \end{cases} \tag{6}$$

and α_s accounts for discontinuous wrapping:

$$\alpha_\mathrm{s} = \left(1 - \frac{s_\mathrm{f}}{2b}\right)\left(1 - \frac{s_\mathrm{f}}{2h}\right) \tag{7}$$

where s_f is the clear vertical spacing between FRP strips and w_f is the strip width, such that $s_\mathrm{f}/w_\mathrm{f} = 0$ for continuous wrapping. Finally, α_a accounts for the fiber orientation effect:

$$\alpha_\mathrm{a} = \frac{1}{1+(\tan\beta_\mathrm{f})^2} \tag{8}$$

where $\beta_{\rm f}$ is the inclination angle of the fibres measured with respect to the column axis.

Material partial factors are defined as $\gamma_{\rm c} = 1.5$ for concrete (yielding $f_{\rm cd} = f_{\rm ck}/\gamma_{\rm c}$) and $\gamma_{\rm f} = 1.25$ for FRP material. A confinement effectiveness threshold requires $f_{\rm l}/f_{\rm cd} \geq 0.07$ for the strength enhancement to be considered.

2.2.2. *ACI 440.2R-17*

The ACI 440.2R-17 guidelines [3] employ a shape factor κ_a similar to $f$ib but utilize a simpler strength model:

$$f_{\rm ccd} = 0.85\phi(f_{\rm ck} + \psi_{\rm f} \cdot 3.3 \cdot \kappa_a \cdot f_{\rm l}) \tag{9}$$

$$\kappa_a = 1 - \frac{(b-2r_{\rm c})^2 + (h-2r_{\rm c})^2}{3A_g}\left(\frac{b}{h}\right)^2 \tag{10}$$

$$D^* = \sqrt{b^2+h^2} \quad \text{(for rectangular sections)} \tag{11}$$

where $\psi_{\rm f} = 0.95$ is an additional reduction factor, and $\phi = 0.65$ is the strength reduction factor, effectively introducing compounded conservatism. ACI also enforces a strict minimum confinement threshold of $f_{\rm l}/f_{\rm ck} \geq 0.08$.

2.2.3. *Proposed Reliability-Based Design (RBD) Model*

The unified generalised model by Mohammadi et al. (2025) was calibrated against a database of 2,117 specimens:

$$f_{\rm ccd} = \phi(s) f_{\rm ck}\left[1 + \frac{3.2\beta_0}{\beta_{\rm UF}} K_{\rm L}^{0.91} f_{\rm ck}^{-1.32} \varepsilon_{\rm fu}^{0.67}\right] \tag{12}$$

where $K_{\rm L}$ is the $2t_{\rm f}E_{\rm f}/D^*$. In this model, D^* is defined as D for circular sections and b for non-circular sections.

$$\beta_0 = \frac{f_{\rm ck}}{15} \leq 1.0 \tag{13}$$

$\beta_{\rm UF}$ is defined as:

$$\beta_{\rm UF} = \beta_{\rm SE} \cdot \beta_R \cdot \beta_\lambda \cdot \beta_P \tag{14}$$

aggregates penalties for size effects ($\beta_{\rm SE}$), shape ($\beta_{\rm R}$), aspect ratio (β_λ), and partial wrapping ($\beta_{\rm P}$):

$$\beta_{\rm SE} = \left(\frac{b}{150}\right)^{0.2} \leq 1.1 \tag{15}$$

$$\beta_{\rm R} = 0.85\left(\frac{2r_{\rm c}}{b}\right)^{-0.75} \geq 1.0 \tag{16}$$

$$\beta_\lambda = \left(\frac{h}{b}\right)^{2.2} \leq 4.0 \tag{17}$$

$$\beta_{\rm P} = 0.7 + 1.8\frac{s_{\rm f}}{w_{\rm f}} \geq 1.0 \tag{18}$$

Critically, this model employs variable resistance factors:

$$\phi(s) = \frac{13.8}{87.7+s} + 0.6 \quad \text{for } s < 175 \tag{19}$$

where $s = K_{\rm L}/f_{\rm ck}$ is the normalized confinement stiffness. This formulation allows less conservative factors in high-confinement, ductile regimes, while maintaining strict safety in brittle, low-confinement zones.

3. Environmental and Economic Assessment Framework

3.1. *Case Study Definition*

Three representative column geometries were analysed:

- **Circular:** $D = 400$ mm
- **Square:** $b = h = 350$ mm, $r_{\rm c} = 30$ mm
- **Rectangular:** $b = 400$ mm, $h = 500$ mm, $r_{\rm c} = 30$ mm

All columns have a height of $H = 3000$ mm and unconfined concrete strength of $f_{\rm ck} = 30$ MPa. The target design strength $f_{\rm target}$ was varied from the baseline ($f_{\rm cd} = f_{\rm ck}/1.5 = 20$ MPa per EN 1992-1-1 [4]) to a maximum of $2f_{\rm cd}$ (100% improvement) in increments of 1%, representing a comprehensive range of strengthening scenarios.

Two commercial CFRP sheets were checked for the best choice to provide each required improvement:

- SikaWrap-230C: $t_{\rm ply} = 0.129$ mm, \$27 per m^2
- SikaWrap-300C: $t_{\rm ply} = 0.167$ mm, \$35 per m^2

Material properties: $E_{\rm f} = 230$ GPa, $\varepsilon_{\rm fu} = 1.7\%$, $\rho_{\rm f} = 1600$ kg/m^3.

3.2. *Life-Cycle Assessment (LCA)*

The environmental impact was evaluated following ISO 14040:2006 and ISO 14044:2006 standards [5, 6], using a "cradle-to-grave" system boundary that encompasses raw material extraction, manufacturing, transportation, installation, and end-of-life disposal. The primary environmental indicator assessed is Global Warming Potential (GWP) in kg CO_2-equivalent. For this comparative study, the focus is on the production and installation phases, as these represent the primary differentiators between design approaches. The operational phase (use) has minimal environmental impact difference since both approaches result in structurally equivalent confined columns. End-of-life impacts are also considered equivalent, as both approaches use identical FRP materials with similar disposal scenarios.

Carbon Fibre Production: Production of carbon fibres is energy intensive, with significant associated greenhouse gas emissions [7]. A conservative value of 54.0 kg CO_2e/kg was adopted to account for high-modulus fibres.

Resin Consumption and Cost: Resin consumption was estimated at 0.7 kg/m^2 per layer (including primer) based on manufacturer data for wet layup systems (e.g., Sikadur-330). The cost of epoxy resin was assumed to be $35/kg. The GWP of the resin was taken as 5.2 kg CO_2e/kg [8].

Composite GWP: The total GWP was calculated by summing the contributions of the dry carbon fibre and the epoxy resin separately:

$$\text{GWP}_{\text{total}} = M_{\text{fiber}} \times 54.0 + M_{\text{resin}} \times 5.2 \quad (20)$$

where M_{fibre} and M_{resin} are the masses of the fibre and resin, respectively.

3.3. *Economic Assessment: Initial Cost Analysis*

The economic evaluation focuses exclusively on initial capital costs for material acquisition, surface preparation, and installation [9]. This is not a complete life-cycle cost analysis (LCCA), as post-installation costs, including maintenance, periodic Rehabilitation and end-of-life disposal are not included. Total initial installed cost includes:

Surface Preparation: $25 per m^2 for sandblasting/grinding.

Corner Rounding: $15 per linear meter for rectangular/square sections (required to achieve r_c of 30 mm).

Material and Labor:

$$C_{\text{mat+lab}} = A_{\text{eff}} \times C_{\text{sheet}} \times (1 + R_L) \quad (21)$$

where A_{eff} accounts for overlaps (200 mm for last layer) and $R_L = 1.5$ is the labour cost ratio, adopted as a conservative estimate for manual wet-layup installation where labour costs typically exceed material costs due to surface preparation and application complexity.

Total Cost:

$$C_{\text{total}} = C_{\text{prep}} + C_{\text{round}} + C_{\text{mat+lab}} \quad (22)$$

For each geometry and target strength, the optimisation algorithm selects the sheet type and number of layers that minimizes total cost while satisfying:

$$f_{\text{ccd}} \geq f_{\text{target}} \quad (23)$$

4. Results and Discussion

4.1. *Material Efficiency*

Figure 1 presents the cost and material comparison for circular columns. As can be seen in the figure, at $f_{\text{target}} \geq 22.6$ MPa, *f*ib and ACI consistently require more thickness of FRP sheets, therefore higher cost. It can be seen that the RBD model costs 12–100% less than *f*ib and 27–100% less than ACI.

Circular Sections: At $f_{\text{target}} \leq 22.6$ MPa: *f*ib and ACI require 2 layers, whereas the RBD model requires 0 layers (100% cost savings), correctly identifying that standard confinement is unnecessary since the unconfined strength is sufficient given the less conservative partial factors.

At $f_{\text{target}} > 22.6$ MPa, *f*ib and ACI consistently require more thickness of FRP sheets, therefore higher cost. It can be seen that the RBD

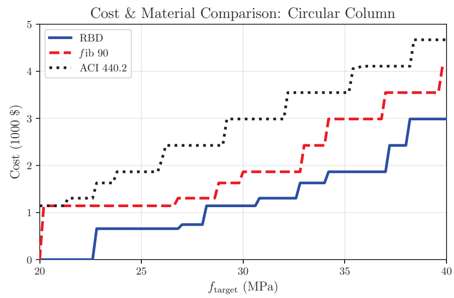

Fig. 1. Cost and material comparison for circular columns

model costs 12-50% less than *f*ib and 27-73% less than ACI.

The total FRP thickness (shown on the secondary axis) demonstrates the material efficiency directly. For example, at $f_{target} = 27$ MPa, *f*ib requires 0.334 mm total thickness (2 layers × 0.167 mm), while RBD achieves the target with 0.167 mm (1 layer).

Square Sections: Figure 2 reveals that geometric inefficiency reduces but does not eliminate the advantage.

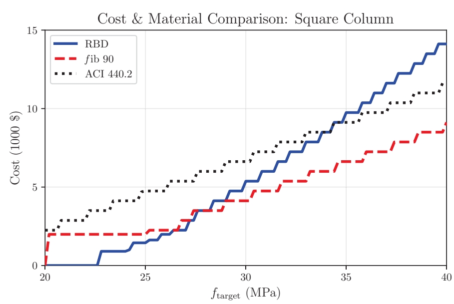

Fig. 2. Cost and material comparison for square columns

At moderate target strengths ($f_{target} \approx$ 22.8–26.2 MPa which translates to up to 31% increase in f_{ccd}), RBD achieves 12-54% cost savings compared to *f*ib. At target strengths up to $f_{target} \approx 33.6$ MPa, RBD achieves 7-78% cost savings compared to ACI. However, at higher targets, RBD models show that a higher thickness of FRP sheets is required than *f*ib and ACI, to secure a safe design. Which highlights the inefficiency of the FRP confinement in these ta levels for squared sections.

Rectangular Sections: Figure 3 shows the most geometrically challenging case.

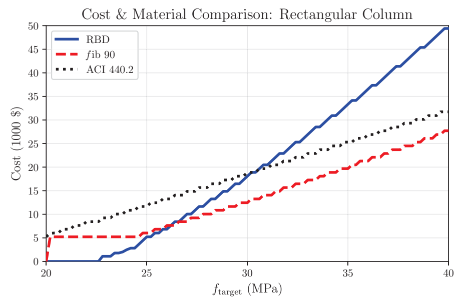

Fig. 3. Cost and material comparison for rectangular columns

The high aspect ratio ($h/b = 1.25$) and relatively small corner radius severely limit confinement effectiveness. The RBD model maintains advantages (yielding 10–79% lower costs) up to approximately $f_{target} \approx 26.2$ MPa, beyond which *f*ib becomes more cost-effective. However, RBD maintains its superiority over ACI 440.2R up to a target strength of 30.6 MPa, with 4–88% cost savings.

4.2. *Environmental Impact*

Figures 4, 5, and 6 presents the GWP comparisons, which closely parallel The cost trends since material volume is the dominant driver.

Circular Sections: A GWP savings of 16–100% compared to *f*ib and 28–100% compared to ACI models was achieved using the RBD model. As a tangible example, consider a retrofit scenario for 50 circular columns ($D = 400$ mm, $H = 3$ m) targeting a design strength of 27 MPa (35% increase):

- ***f*ib Model:** ≈ 8.1 tonnes CO_2e
- **Proposed RBD Model:** ≈ 4.3 tonnes

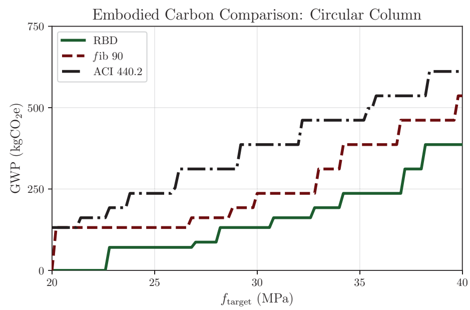

Fig. 4. GWP comparison for circular columns

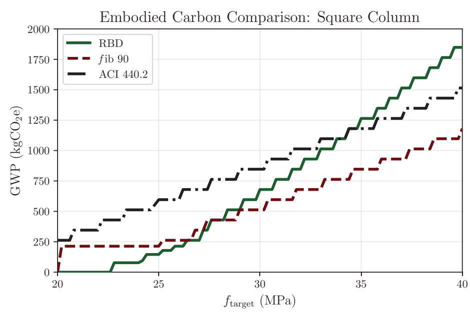

Fig. 5. GWP comparison for square columns

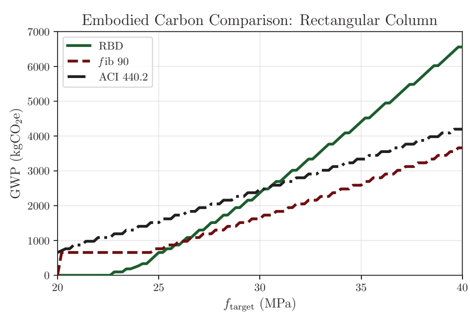

Fig. 6. GWP comparison for rectangular columns

CO_2e

This results in an avoided burden of 3.8 tonnes CO_2e for this single project.

Square Sections: GWP savings of 19-100% for targets up to 26.2 MPa in *f*ib model and 8-100% in ACI model for targets up to 33.6 MPa are achieved, While for higher strength targets the RBD model requires more thickness of FRP sheets, therefore higher cost.

Rectangular Sections: GWP savings of 12-100% for targets up to 26.2 MPa in *f*ib model and 9-100% in ACI model for targets up to 33.6 MPa are achieved, while for higher strength targets, the RBD model requires more thickness of FRP sheets, therefore higher cost.

4.3. *Cross-Geometry Performance*

Figure 7 quantifies the cost penalty of non-circular shapes relative to circular sections using the all model.

The cost ratio (Square/Circular or Rectangular/Circular) provides design guidance:

- **Square sections:** The cost multiplier ranges from approximately 1.4 to over 5.0 across the models and improvement levels, indicating a substantial premium for strengthening square columns.
- **Rectangular sections:** The geometric inefficiency is most pronounced here, with cost multipliers starting at 1.6 but reaching upwards of 15.0–18.0 for the RBD model at high strengthening targets, while conventional codes (*f*ib and ACI) generally show multipliers in the 5.0–7.0 range.

This pronounced penalty in the RBD model is mechanically grounded in the non-uniformity of confinement pressure characteristic of non-circular sections, where effective confinement is limited to the corners due to arching action. This geometric effect introduces significant model uncertainty compared to the uniform confinement of circular sections. The reliability analysis calibrated by Mohammadi et al. [1] explicitly quantified this uncertainty, demonstrating that to achieve the same target reliability index (β_T) as circular columns, significantly higher penalising factors are required for rectangular geometries. Thus, the increased material demand is a direct outcome of enforcing consistent safety levels across substantially different confinement mechanisms.

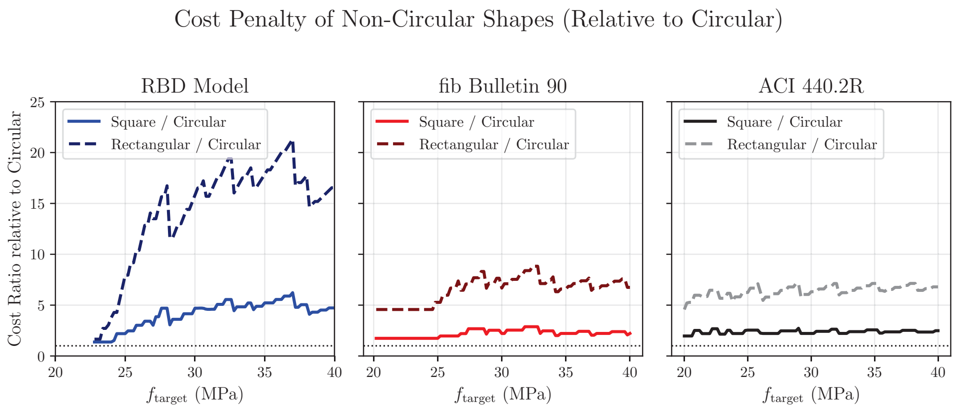

Fig. 7. Cost penalty of non-circular shapes relative to circular sections

This analysis highlights the economic incentive to maximize corner radius and avoid strengthening columns with high aspect ratios using FRP confinement.

4.4. *Practical Implications*

Design Recommendations:

(1) For circular columns requiring *any* level of strengthening, the RBD model provides substantial material and cost savings while maintaining target reliability
(2) For square/rectangular columns with moderate strengthening needs (<30-35% improvement), RBD offers meaningful advantages
(3) For heavily loaded rectangular columns requiring >40% improvement, geometric inefficiency dominates; consider using other strengthening methods

Sustainability Context: The construction sector accounts for approximately 38% of global CO_2 emissions [10]. While FRP materials have higher embodied carbon per kg than traditional materials, their application in strengthening avoids the far greater emissions associated with demolition and reconstruction. The 30-50% material reduction achieved by RBD optimisation amplifies this benefit.

Consider a hypothetical retrofit project strengthening 50 circular columns:

- Using *f*ib Bulletin 90: ∼122 kg carbon fiber (plus resin) → 8.1 tonnes CO_2e
- Using RBD: ∼61 kg carbon fiber (plus resin) → 4.3 tonnes CO_2e
- **Emissions avoided:** 3.8 tonnes CO_2e

This savings is equivalent to the embodied carbon of approximately 11 m^3 of standard C30/37 concrete (approx. 26 tonnes), effectively offsetting the carbon footprint of a significant portion of the structural elements being managed.

5. Conclusions

This study quantified the environmental and economic implications of adopting reliability-based design (RBD) for FRP-confined concrete columns. Key findings include:

(1) The RBD model achieves 16–100% cost and GWP savings for circular columns compared to *f*ib Bulletin 90, and 28–100% compared to ACI 440.2R, demonstrating its high efficiency for this geometry.
(2) For square and rectangular sections, the RBD model offers 19–100% and 12–100% savings, respectively, at moderate strengthening levels (up to ≈ 26 MPa). However, at higher strength targets, the RBD model correctly identifies the geometric inefficiency and requires more

material than conventional codes to maintain the target reliability index ($\beta_T = 3.8$).

(3) Geometric efficiency is a critical driver of cost and sustainability. Rectangular sections with high aspect ratios exhibit cost multipliers of up to $18\times$ relative to circular columns in the RBD model, significantly higher than the $\approx$ 5–7$\times$ suggested by deterministic codes.

(4) The use of variable resistance factors $\phi(s)$ allows for rigorous optimisation where physics permits (circular, low-eccentricity) while enforcing necessary conservatism where confinement physics is weak (sharp corners, high aspect ratios).

(5) This approach supports a transition to sustainable infrastructure by encouraging efficient geometric design and providing accurate, reliability-consistent incentives for material saving.

The findings validate that reliability-informed design is not merely a safety calibration exercise, but a pathway toward sustainable, economically viable infrastructure renewal.

It is important to acknowledge the boundaries of applicability for the models assessed in this study. These results are strictly valid for short columns under concentric axial compression. Effects of load eccentricity and slenderness, which reduce confinement efficiency, are not explicitly covered. Additionally, the interaction between internal longitudinal reinforcement and high confinement levels (e.g., bar buckling) requires further investigation.

Acknowledgement

The authors acknowledge the support provided by the Institute for Sustainability and Innovation in Structural Engineering (ISISE) and funding from the Portuguese Foundation for Science and Technology (FCT).

References

1. Amirhossein Mohammadi, Javad Shayanfar, and Joaquim A. O. Barros. Reliability-based design model for compressive strength of axially loaded FRP-confined concrete columns. *Composite Structures*, 2025. doi: 10.1016/j.compstruct.2025.xxxxx. In press.
2. *f*ib Task Group 9.3. Externally applied FRP reinforcement for concrete structures. Bulletin 90, Fédération Internationale du Béton (fib), Lausanne, Switzerland, 2019.
3. ACI Committee 440. *Guide for the Design and Construction of Externally Bonded FRP Systems for Strengthening Concrete Structures (ACI 440.2R-17)*. American Concrete Institute, Farmington Hills, MI, 2017.
4. European Committee for Standardization. Eurocode 2: Design of concrete structures - part 1-1: General rules and rules for buildings. European Standard EN 1992-1-1:2004, CEN, Brussels, Belgium, 2004.
5. International Organization for Standardization. Environmental management life cycle assessment principles and framework. International Standard ISO 14040:2006, ISO, Geneva, Switzerland, 2006.
6. International Organization for Standardization. Environmental management life cycle assessment requirements and guidelines. International Standard ISO 14044:2006, ISO, Geneva, Switzerland, 2006.
7. Robert A. Witik, Remy Teuscher, Véronique Michaud, Christian Ludwig, and Jan-Anders E. Månson. Carbon fibre reinforced composite waste: An environmental assessment of recycling, energy recovery and landfilling. *Composites Part A: Applied Science and Manufacturing*, 49: 89–99, 2013. doi: https://doi.org/10.1016/j.compositesa.2013.02.009.
8. Mads Juhl, Michael Z Hauschild, and Kim Dam-Johansen. Assessing the environmental sustainability of lignin-based epoxy resins for coating production. *ACS Sustainable Chemistry & Engineering*, 12(12):4970–4978, 2024.
9. Vistasp M. Karbhari. *Durability of Composites for Civil Structural Applications*. Woodhead Publishing, Cambridge, UK, 2007. ISBN 978-1-84569-035-8.
10. Circular Ecology. Inventory of carbon and energy (ICE) database v4.1. `https://www.circularecology.com`, 2025.